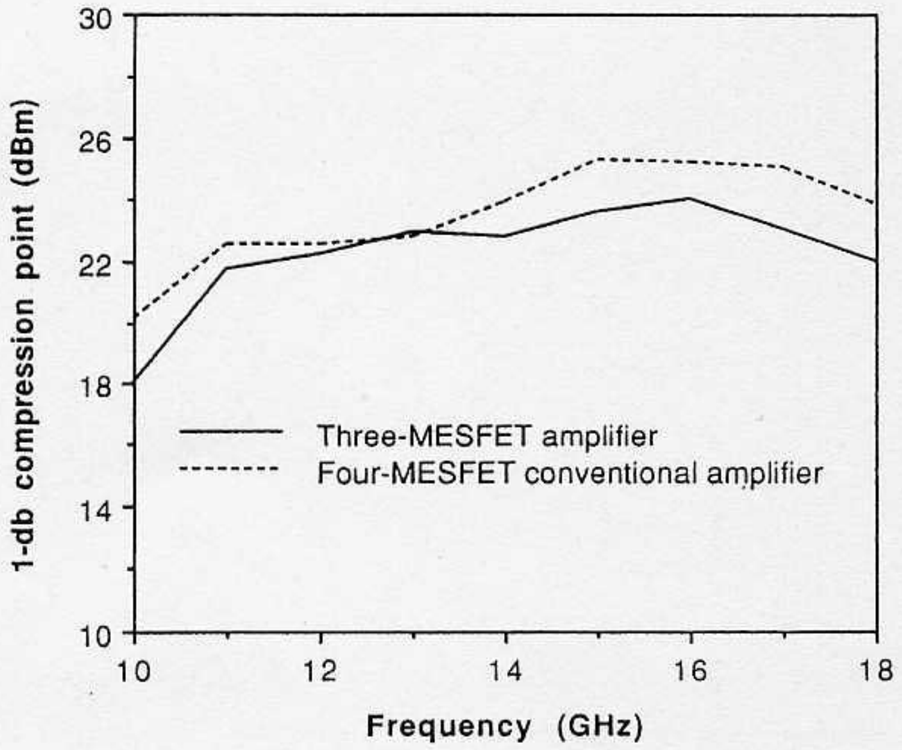


**Figure 5** Comparison of the 1-dB compression point as a function of the frequency

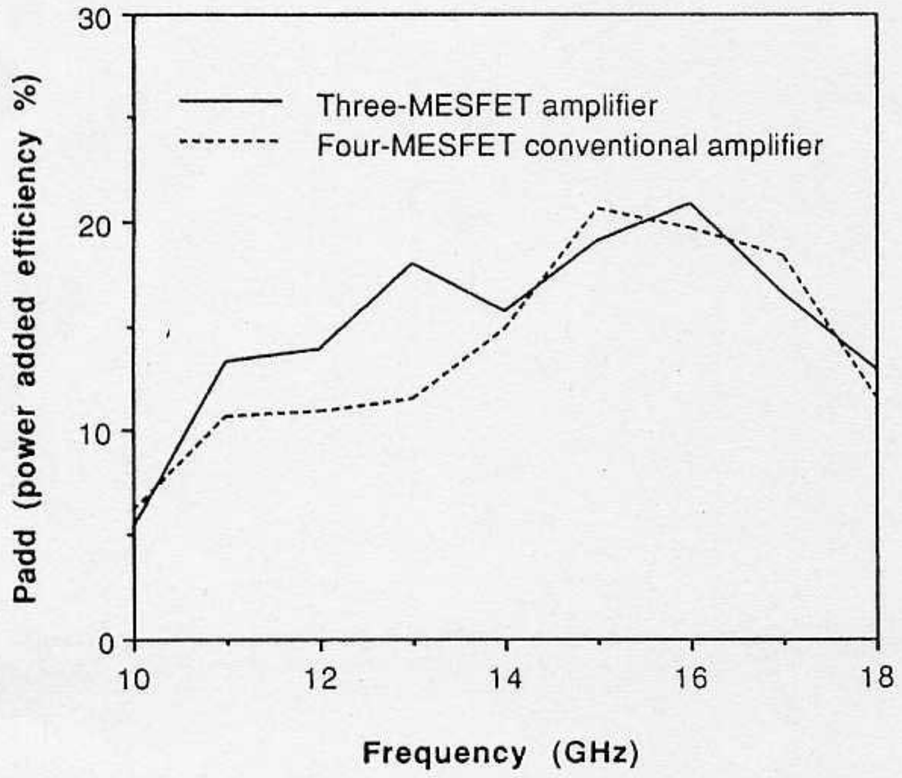


**Figure 6** Comparison of the power-added efficiency, $P_{add}$, as a function of the frequency

ber of MESFETs makes this amplifier attractive to designers, who can choose from a wider range of performance, as was demonstrated in the presented application.

## REFERENCES

1. N. B. Kim, H. Q. Tserng, and H. D. Shih, "Ka-Band Monolithic GaAs FET Power Amplifier Modules," in *Proceedings of the IEEE Millimeter Wave Monolithic Circuit Symposium*, 1988, pp. 129–132.
2. M. Gat, "Ku-Band 8 W MMIC Power Amplifier," *IEEE MTT-S International Microwave Symposium Digest*, 1991, pp. 1299–1302.
3. K. B. Niclas, R. R. Pereira, and A. P. Chang, "On Power Distribution in Additive Amplifier," *IEEE Trans. Microwave Theory Tech.*, Vol. MTT-38, 1990, pp. 1692–1699.
4. J. B. Beyer, S. N. Prasad, R. C. Becker, J. E. Nordman, and G. K. Hohenwarter, "MESFET Distributed Amplifier Guidelines," *IEEE Trans. Microwave Theory Tech.*, Vol. MTT-32, 1984, pp. 268–275.
5. S. D'Agostino and C. Paoloni, "An Innovative Power Distributed Amplifier Using the Wilkinson Combiner," *IEE Proc. Microwave Antennas Propagat.*, to be published.

*Received 3-14-95*

Microwave and Optical Technology Letters, 9/6, 310–312

CCC 0895-2477/95

# ELIMINATION OF THE SPURIOUS ROOT IN THE SDA SOLUTION TO THE SHIELDED MICROSTRIP PROBLEM

**Smain Amari and Jens Børnemann**
Laboratory for Lightwave Electronics, Microwaves and Communications
LLiMiC
University of Victoria
Victoria, British Columbia, Canada V8W 3P6

**KEY TERMS**

*Spectrum-domain method, shielded microstrip, numerical method*

**ABSTRACT**

*We report that the spurious root that appears in the spectral-domain approach solution to the shielded lossless and infinitely thin microstrip is eliminated when enough basis functions to accurately describe the transverse current density are used. A fast algorithm based on the observed simple behavior of the minimum singular value of the characteristic matrix as a function of $\beta^2$ instead of $\beta$ is presented. For lossless microstrip lines, with small values of the dielectric constant and at relatively low frequencies, two evaluations of the characteristic matrix are sufficient to determine its dispersion properties, when the longitudinal current density is assumed Maxwellian, thus achieving a considerable reduction of CPU time.* © *1995 John Wiley & Sons, Inc.*

## 1. INTRODUCTION

Recent years have seen an increasing interest in developing methods to eliminate nonphysical solutions that appear in computer simulation of physical phenomena. For the transverse resonance method as applied to planar circuits, Aubert, Souny, and Baudrand [1] showed that the choice of transverse and longitudinal basis functions, which are not independent of each other, eliminates the nonphysical roots, whose origin is traced back to the inadequate treatment of the infinite-$\beta$ solution. For the method of moments, Schroeder and Wolff [2] examined the effect of discretization on the appearance of nonphysical solutions of linear homogeneous eigenvalue problems. The finite-element method also suffers from similar pathologies, and there is an extensive literature discussing the techniques developed in recognizing and eliminating the spurious roots [3, 4]. The spectral-domain approach (SDA), when applied to the solution of the shielded lossless microstrip problem, has been known for some time to lead to a nonphysical root for the effective dielectric constant at $(\varepsilon_r + 1)/2$. This root was also reported by Daly [5] in the finite-element solution. Krage and Haddad [6] also reported the appearance of this root. Jansen [7] proposed a choice of basis functions that are twice continuously differentiable in order to avoid spurious roots such as those reported by Farrar and Adams [8].

This short article focuses exclusively on the spurious root in the spectral-domain approach. We show that the contribution of the transverse current density is essential to the elimination of this root. We also present a simple and extremely fast scheme to determine the dispersion properties of the lossless microstrip line.

## 2. SPURIOUS ROOT OF A SHIELDED MICROSTRIP

We consider a shielded, lossless, and infinitely thin microstrip line as shown in the inset of Figure 1. The structure is infinitely long in the $z$ direction, and we assume a harmonic time variation $e^{j\omega t}$ and propagation in the $z$ direction $e^{-j\beta z}$,

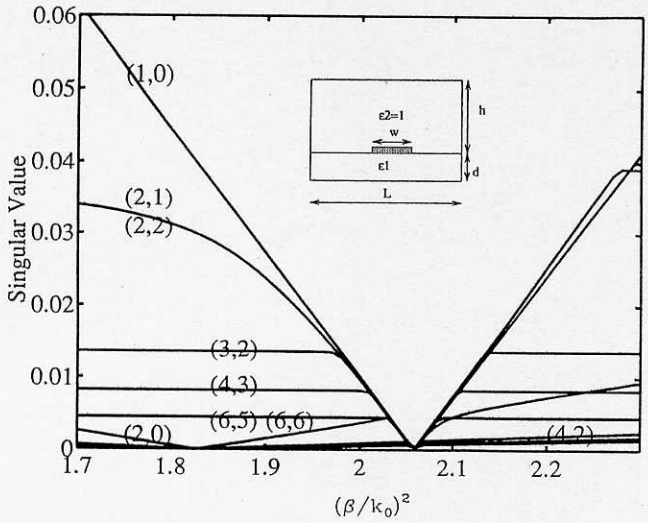


**Figure 1** Minimum singular value $\Sigma$ as a function of $(\beta/k_0)^2$ for $\varepsilon = 2.65$, $d = 1.27$ mm, $w = 1.27$ mm, $h = 11.43$ mm, $l = 12.7$ mm, and different values of $n_x$ and $n_z$ at 1 GHz. Note the piecewise linearity of the curve for $n_z = 1$

$\beta$ is the unknown propagation constant of the dominant even mode.

Following the spectral-domain approach [9, 10], the Green's impedance dyadics of the system are found to be

$$\begin{pmatrix} \tilde{E}_x \\ \tilde{E}_z \end{pmatrix} = \begin{pmatrix} Z_{xx} & Z_{xz} \\ Z_{zx} & Z_{zz} \end{pmatrix} \begin{pmatrix} \tilde{J}_x \\ \tilde{J}_z \end{pmatrix}, \tag{1}$$

where $\tilde{E}_{x,z}$ is the Fourier transform of the tangential electric field at the interface, and the elements $Z_{ij}$ are given by

$$Z_{xx} = \frac{1}{\alpha^2 + \beta^2}\left[\frac{\alpha^2}{Y_1^{\mathrm{LSM}} + Y_2^{\mathrm{LSM}}} + \frac{\beta^2}{Y_1^{\mathrm{LSE}} + Y_2^{\mathrm{LSE}}}\right], \tag{2a}$$

$$Z_{xz} = G_{zx} = \frac{\alpha\beta}{\alpha^2 + \beta^2}\left[\frac{1}{Y_1^{\mathrm{LSM}} + Y_2^{\mathrm{LSM}}} - \frac{1}{Y_1^{\mathrm{LSE}} + Y_2^{\mathrm{LSE}}}\right], \tag{2b}$$

$$Z_{zz} = \frac{1}{\alpha^2 + \beta^2}\left[\frac{\alpha^2}{Y_1^{\mathrm{LSE}} + Y_2^{\mathrm{LSE}}} + \frac{\beta^2}{Y_1^{\mathrm{LSM}} + Y_2^{\mathrm{LSM}}}\right]. \tag{2c}$$

$\alpha = (2n + 1)\pi/2L$ and $\gamma_i^2 = \alpha^2 + \beta^2 - \omega^2\varepsilon_i\varepsilon_0\mu_0$. The admittances $Y_1$ and $Y_2$ for the LSE and LSM modes are given by [11]

$$Y_1^{\mathrm{LSE}} = \frac{j\omega\varepsilon_1\varepsilon_0}{\gamma_1}\coth(\gamma_1 d), \tag{3a}$$

$$Y_1^{\mathrm{LSM}} = \frac{\gamma_1}{j\omega\mu_0}\coth(\gamma_1 d), \tag{3b}$$

$$Y_2^{\mathrm{LSM}} = \frac{\gamma_2}{j\omega\mu_0}\coth(\gamma_2 h), \tag{3c}$$

$$Y_2^{\mathrm{LSE}} = \frac{j\omega\varepsilon_2\varepsilon_0}{\gamma_2}\coth(\gamma_2 h). \tag{3d}$$

In order to understand the origin of the spurious root in the present structure, we focus on the quantity $Z_{zz}$. If the quantities $\gamma_1 d$ and $\gamma_2 h$ are large, which occurs when $\alpha$ is large, we can approximate the hyperbolic functions by unity and the $\gamma$'s by $\alpha$. Carrying out the algebra, $Z_{zz}$ becomes

$$Z_{zz} \to \frac{\alpha}{j\omega\varepsilon_0(\beta^2 + \alpha^2)}\left[\frac{\beta^2}{\varepsilon_1 + 1} - \frac{k_0^2}{2}\right]. \tag{4}$$

From this last equation it is clear that if only the longitudinal current is taken into account, a possible spurious root in the propagation constant at

$$\left(\frac{\beta}{k_0}\right)^2 = \frac{1 + \varepsilon_1}{2} \tag{5}$$

will be encountered. Note that the other terms in the Green's impedance dyadics do not vanish at this value of the propagation constant. Consequently, the inclusion of the transverse current density, which gives nonzero matrix elements containing $Z_{xx}$ and $Z_{zx}$, in the Galerkin solution will prevent this root from occurring.

### 3. ROLE OF TRANSVERSE CURRENT

To obtain the propagation constant of the microstrip, the current density is expanded in a series of functions

$$J_z(x) = \sum_{i=1}^{n_z} c_i f_i(x), \tag{6a}$$

$$J_x(x) = \sum_{i=1}^{n_x} d_i g_i(x). \tag{6b}$$

When Galerkin's method is applied, the expansion coefficients $c_i$ and $d_i$ are found to satisfy a set of linear equations that can be written in a matrix form as

$$[K][X] = 0. \tag{7}$$

Such a linear systems admits a nontrivial solution only if its determinant vanishes, or, equivalently, if one or more of the singular values of the matrix $[K]$ vanish [12].

The current density along an infinitely thin perfect conductor is singular at the edges; consequently the following functions are used to represent the longitudinal and transverse currents, respectively:

$$f_n(x) = \frac{\cos\left(\dfrac{4n\pi x}{w}\right)}{\sqrt{1 - \left(\dfrac{2x}{w}\right)^2}}, \qquad n = 0, 1, \ldots, \tag{8a}$$

$$g_n(x) = \frac{\sin\left(\dfrac{2n\pi x}{w}\right)}{\sqrt{1 - \left(\dfrac{2x}{w}\right)^2}}, \qquad n = 1, 2, \ldots. \tag{8b}$$

The Fourier transforms of $f_n$ and $g_n$ are expressible in terms of Bessel functions of order zero [13]. Figure 1 shows the

minimum singular value $\Sigma$ of the matrix $[K]$ for different values of $n_x$ and $n_z$ as a function of $(\beta/k_0)^2$. It is interesting to note that only one solution appears when $n_z = 1$ and $n_x = 0$ when $d = 1.27$ mm. In this case the lower terms in the inner product $\Sigma_n Z_{zz}|\tilde{J}_z(\alpha_n)|^2$ do not have the factor $\beta^2/(1 + \varepsilon_1) - k_0^2/2$ and are large enough to prevent the spurious root from appearing. If, however, $d$ is increased to 5 mm, the spurious root is found again at the same location, because the conditions that led to Eq. (4) are better satisfied for a thick substrate ($\gamma_1 d$ large). In other words, when the substrate is thick enough, the hyperbolic functions that appear in $Z_{zz}$ can be approximated by unity, even for small values of $\alpha_n$ (or large $L$), thereby allowing the quantity $\beta^2/(1 + \varepsilon_1) - k_0^2/2$ to be factored out. If $n_z = 2$, two roots are found, one of them at $(\varepsilon_1 + 1)/2$ if $n_x = 0$, and only one if $n_x \geq 1$. The results are summarized in Table 1 for $d = 1.27$ mm. It is clearly seen that the spurious root is always eliminated if a sufficient number of terms in the transverse current density is used. The absence of the spurious root for $n_z = 1$, $n_x = 0$, and its presence when $n_z = 2$, $n_x = 0$, is due to the fact that the determinant is a difference between the products of the diagonal and the off-diagonal elements. It is straightforward to check that this leads to cancellation of the dominant terms, which prevented the root from appearing in the case of $n_z = 1$, $n_x = 0$.

Note also the simple behavior of $\Sigma$ when $n_z = 1$. This practically linear dependence on $(\beta/k_0)^2$ means that very few evaluations of the matrix $[K]$ are needed to obtain the dispersion relation of the shielded lossless microstrip. Figure 2 shows the dispersion relation as obtained from a piecewise linear approximation of the minimum singular value as a function of $(\beta/k_0)^2$ and not $\beta$. This simple change of variable is sufficient to linearize $\Sigma(\beta)$ especially at low frequencies and small values of the dielectric constant. For $\varepsilon_1 = 2.65$, only two evaluations of the matrix $[K]$ per frequency point were needed to generate the curve up to 20 GHz. The corresponding CPU time is 0.24 s per frequency point on a RISC 6000/530 workstation. The crosses in Figure 2 show that our results obtained through this simple scheme agree well with the quoted data [14]. If the dielectric constant is increased to 8.875, $\Sigma$ starts to deviate from the piecewise linearity at 15 GHz. At 40 GHz, four iterations were needed for the scheme to converge.

## 4. CONCLUSIONS

The spurious root, which appears in the spectral-domain approach's solution to the shielded lossless microstrip line, is shown to be eliminated by an adequate representation of the transverse current density. The simple dependence of the minimum singular value of the characteristic matrix on $(\beta/k_0)^2$ can be used to determine the dispersion of the microstrip with very few evaluations of the characteristic matrix, thereby considerably reducing CPU time.

**TABLE 1 Number of Roots**

| | $n_z$ | | | | | |
|---|---|---|---|---|---|---|
| $n_x$ | 1 | 2 | 3 | 4 | 5 | 6 |
| 0 | 1 | 2 | 2 | 2 | 2 | 2 |
| 1 | 1 | 1 | 2 | 2 | 2 | 2 |
| 2 | 1 | 1 | 1 | 2 | 2 | 2 |
| 3 | 1 | 1 | 1 | 1 | 2 | 2 |
| 4 | 1 | 1 | 1 | 1 | 1 | 2 |
| 5 | 1 | 1 | 1 | 1 | 1 | 1 |
| 6 | 1 | 1 | 1 | 1 | 1 | 1 |

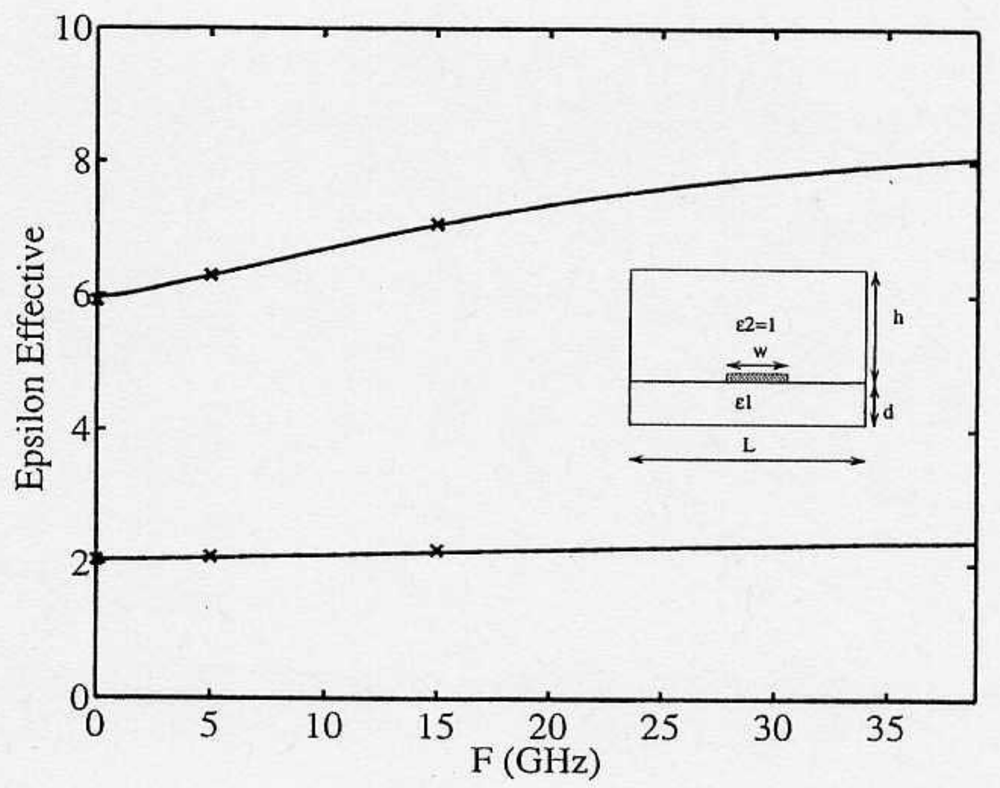


**Figure 2** Dispersion relation of a lossless microstrip as calculated from at most four iterations with a Maxwellian current density. The crosses are from Reference [14]

## REFERENCES


1. H. Aubert, B. Souny, and H. Baudrand, "Origin and Avoidance of Spurious Solutions in the Transverse Resonance Method," *IEEE Trans. Microwave Theory Tech.*, Vol. MTT-41, No. 3, March 1993, pp. 450–456.
2. W. Schroeder and I. Wolff, "The Origin of Spurious Modes in Numerical Solutions of Electromagnetic Field Eigenvalue Problems," *IEEE Trans. Microwave Theory Tech.*, Vol. MTT-42, No. 4, April 1994, pp. 644–653.
3. M. Koshiba, K. Hayata, and M. Suzuki, "Finite-Element Method Analysis of Microwave and Optical Waveguides–Trends in Countermeasures to Spurious Solutions," *Electron. Commun. Jpn. Pt. 2*, Vol. 70, No. 9, 1987, pp. 96–108.
4. B. M. A. Rahman, F. A. Fernandez, and J. B. Davies, "Review of Finite Element Methods for Microwave and Optical Waveguides," *Proc. IEEE*, Vol. 79, No. 10, Oct. 1991, pp. 1442–1448.
5. P. Daly, "Hybrid-Mode Analysis of Microstrip by Finite-Element Methods," *IEEE Trans. Microwave Theory Tech.*, Vol. MTT-19, Jan. 1971, pp. 19–225.
6. M. K. Krage and G. I. Haddad, "Frequency-Dependent Characteristics of Microstrip Transmission Lines," *IEEE Trans. Microwave Theory Tech.*, Vol. MTT-20, Oct. 1972, pp. 678–688.
7. R. H. Jansen, "High-Speed Computation of Single and Coupled Microstrip Parameters Including Dispersion, High-Order Modes, Loss and Finite Strip Thickness," *IEEE Trans. Microwave Theory Tech.*, Vol. MTT-26, Feb. 1978, pp. 75–82.
8. A. Farrar and A. T. Adams, "Computation of Propagation Constants for the Fundamental and Higher Modes in Microstrip," *IEEE Trans. Microwave Theory Tech.*, Vol. MTT-24, July 1976, pp. 456–460.
9. T. Itoh, "Spectral Domain Immittance Approach for Dispersion Characteristics of Generalized Printed Transmission Lines," *IEEE Trans. Microwave Theory Tech.*, Vol. 28, pp. 733–736, July 1980.
10. R. H. Jansen, "The Spectral Domain Approach for Microwave Integrated Circuits," *IEEE Trans. Microwave Theory Tech.*, Vol. MTT-3, Oct. 1985, pp. 1043–1056.
11. D. Mirshekar-Syahkal, *Spectral Domain Method for Microwave Integrated Circuits*, Wiley, New York, 1990.
12. V. A. Labay and J. Bornemann, "Matrix Singular Value Decomposition for Pole-Free Solutions of Homogeneous Matrix Equations as Applied to Numerical Modeling Methods," *IEEE Mi-*

*crowave Guided Wave Lett.*, Vol. MGW-2, No. 2, Feb. 1992, pp. 49–51.
13. T. Itoh (Ed.), *Numerical Techniques for Microwave and Millimeter-Wave Passive Structures*, Wiley, New York, 1989.
14. T. Itoh and R. Mittra, "A Technique for Computing Dispersion Characteristics of Shielded Microstrip Lines," *IEEE Trans. Microwave Theory Tech.*, Oct. 1974, pp. 896–898.

*Received 3-21-95*

Microwave and Optical Technology Letters, 9/6, 312–315

CCC 0895-2477/95

# NUMERICAL DISPERSION IN THE FINITE-ELEMENT METHOD USING TRIANGULAR EDGE ELEMENTS

**Gregory S. Warren**
USAF Rome Laboratory
RL/ERAS
31 Grenier St.
Hanscom AFB, Massachusetts 01731

**Waymond R. Scott, Jr.**
School of Electrical and Computer Engineering
Georgia Institute of Technology
Atlanta, Georgia 30332

**KEY TERMS**

*Finite-element method, triangular mesh, dispersion, wave propagation*

**ABSTRACT**

*The discretization inherent in the finite-element method results in the numerical dispersion of a propagating wave. The numerical dispersion of a time-harmonic plane wave propagating through an infinite, two-dimensional, finite-element mesh composed of uniform triangular edge elements is investigated in this work. The effects on the numerical dispersion of the propagation direction of the wave, the electrical size of the elements, and the mesh geometry are investigated. The dispersion for the hexagonal mesh geometry is shown to be much smaller and to converge at a quicker rate than the other meshes. The dispersion analysis is validated by numerical examples. © 1995 John Wiley & Sons, Inc.*

## I. INTRODUCTION

The finite-element method is a popular technique in computational electromagnetics. Two different approaches are commonly used when applying the finite-element method to solve vector field problems. In both techniques, the domain of interest is divided into subdomains or elements. The difference in the two approaches is in the manner in which the field is approximated within the elements. In the nodal element approach, each component of the field is represented by an expansion of scalar basis functions, whereas, in the edge-element approach, the vector field is approximated by an expansion of vector basis functions. The latter technique offers some significant advantages over the former. For one, it does not suffer from spurious or nonphysical solutions for many types of problems, as does the nodal element approach [1]. In addition, boundary conditions are generally easier to impose along conductor edges and material interfaces when the edge elements are used.

Even though the finite-element method has been extensively used, the errors associated with it have not been thoroughly investigated. A quantification of these errors is important for one to have complete confidence in the numerical solution. One of the most significant errors arises from the inability of the polynomial basis functions to represent the fields exactly within an element. This error is commonly called the discretization error and is present when nodal elements or vector elements are utilized. A wave propagating through a mesh of finite elements will experience numerical dispersion as a result of this error.

Most research into the numerical dispersion of plane waves propagating through finite element meshes has concentrated on meshes composed of nodal elements [2–5]. The research into the numerical dispersion of edge-element meshes is not as extensive. The authors have investigated the numerical dispersion for quadrilateral, edge-element meshes [6]. Monk and Parrott have investigated the numerical dispersion of several types of triangular elements for a finite-element time-domain method for Maxwell's equations. Their method uses a separate mesh to approximate the electric field and the magnetic field [7].

In this work, the numerical dispersion of a time-harmonic plane wave propagating through a number of infinite, two-dimensional, finite-element meshes composed of triangular edge elements is investigated. The numerical dispersion is characterized by a cumulative phase error. The phase error is quantified as a function of the electrical size of the elements, the direction of propagation of the plane wave, and the orientation of the elements. Results are given that can serve as a guide in selecting the appropriate element size and mesh geometry. The phase error for the hexagonal mesh is demonstrated to be significantly smaller and to converge quicker than the phase error for the other meshes. Finally, numerical results that verify the analysis are given.

## II. DISPERSION ANALYSIS

In order to quantify the numerical dispersion of the vector finite-element method, consider an infinite, linear, two-dimensional, homogeneous, isotropic, and source-free region. The field in this region is governed by the vector Helmholtz equation:

$$\nabla \times (\nabla \times \mathbf{E}) - k^2 \mathbf{E} = 0, \tag{1}$$

where an $e^{j\omega t}$ time dependence is assumed and $k = \omega\sqrt{\mu\epsilon}$ is the wave number.

It is well known that a plane wave is an exact solution to the vector Helmholtz equation (1). For the plane-wave solution, the field at any point $p$ is related to the field at any other point $q$ by a simple phase factor:

$$\mathbf{E}_q = \mathbf{E}_p e^{-jk\hat{k}\cdot\Delta\mathbf{r}}, \tag{2}$$

where $\hat{k} = \cos\phi\hat{a}_x + \sin\phi\hat{a}_y$ is a unit vector pointing in the direction of propagation and where $\Delta\mathbf{r}$ is the vector from point $p$ to point $q$.

Now consider dividing the region into an infinite, uniform mesh. The field in this mesh will be governed by a discretized vector Helmholtz equation. A plane wave propagating along the mesh at an angle $\phi$ is a solution to the discretized vector Helmholtz equation as well. However, the plane wave propagates with a numerical wave number $\tilde{k}$ that differs from the analytical wave number $k$.

Consider the points $p$ and $q$ depicted in the mesh in Figure 1. The relationship between the discretized field at